Ionization-potential depression and dynamical structure factor in dense plasmas

Chengliang Lin,[1,*] Gerd Röpke,[1,†] Wolf-Dietrich Kraeft,[1,‡] and Heidi Reinholz[1,2,§]
[1]*Universität Rostock, Institut für Physik, 18051 Rostock, Germany*
[2]*University of Western Australia School of Physics, WA 6009 Crawley, Australia*
(Received 9 March 2017; published 6 July 2017)

The properties of a bound electron system immersed in a plasma environment are strongly modified by the surrounding plasma. The modification of an essential quantity, the ionization energy, is described by the electronic and ionic self-energies, including dynamical screening within the framework of the quantum statistical theory. Introducing the ionic dynamical structure factor as the indicator for the ionic microfield, we demonstrate that ionic correlations and fluctuations play a critical role in determining the ionization potential depression. This is, in particular, true for mixtures of different ions with large mass and charge asymmetry. The ionization potential depression is calculated for dense aluminum plasmas as well as for a CH plasma and compared to the experimental data and more phenomenological approaches used so far.

DOI: 10.1103/PhysRevE.96.013202

I. INTRODUCTION

In the context of new experimental facilities exploring warm dense matter (WDM) and materials in the high-energy density regime, a detailed theoretical investigation of thermodynamic, transport, and optical properties of strongly coupled and nearly degenerate Coulomb systems becomes of emerging interest. This is of relevance not only for material science investigating matter under extreme conditions (Mbar pressures, temperatures of 1 eV up to 1 keV), like inertial confinement fusion implosions in laboratory experiments, but also for understanding the structure and evolution of the increasing number of known planets as well of other astrophysical objects.

A fundamental phenomenon is the modification of bound-state levels as well as of continuum states owing to the surrounding warm and dense medium. Here, we are interested in the ionization potential depression (IPD), which is relevant for the composition of the plasma, and, in this way, for the thermodynamic and transport properties. We focus on experiments showing the dissolution of spectral lines due to the IPD which determines the ionization degree of WDM. Accurate predictions are necessary for simulation codes such as FLYCHK [1] which model plasmas under extreme conditions.

Being a long-standing problem in plasma physics, IPD experiments [2–7] have been performed recently using the new possibility to produce highly excited plasmas at condensed matter densities by intense short-pulse laser irradiation. Comparisons of observed optical spectra with simulations using traditional expressions for the IPD given by Ecker and Kröll (EK) [8] or Stewart and Pyatt (SP) [9] have been performed. Neither of them leads to a satisfying description for all of the available experiments. While, on one hand, Hoarty's results [2] on the disappearance of spectral lines seem to favor SP, and, on the other hand, the direct measurements on the ionization energy of the K-shell in aluminum and the subsequent K_α lines by Ciricosta *et al.* [3,4] tend to confirm EK, recently reported results by Kraus *et al.* [7] cannot be understood by either of the two approaches. A more systematic and accurate theory is demanded to describe the measurements.

The commonly used expressions for the IPD derived by Ecker and Kröll [8] or Stewart and Pyatt [9] interpolate between the Debye (DH) limit for low densities and an ion sphere (IS) expression, see Ref. [10], for high densities. They are based on simplified assumptions such as the introduction of an average static potential to perform Thomas-Fermi calculations. A critical discussion of these approaches and their applicability for the experiments given above was presented in Ref. [11]. Other approaches use Hartree-Fock-Slater calculations [12], Monte Carlo simulations [13], molecular dynamics simulations [14], density-functional theory calculations [15], microfield concepts and a detailed configuration accounting description [17,18], or the theory of disordered solids where itinerant band electrons become localized below a mobility edge [19].

A systematic approach to describe the properties of dense plasmas is given by the quantum statistical many-body theory, in particular the use of the Green function method [20]. It has been applied to optical properties [21] by calculating shifts and broadening of spectral lines in a plasma environment. The shift of bound states and the continuum edge in dense plasmas has also been considered in Refs. [22–24].

Already some decades ago, the shifts both of the continuum edge and of the bound-state levels have been discussed for the electron-hole plasma in excited semiconductors [20,23–26]. Depending on the density and temperature of the electron-hole plasma, excitons are modified by medium effects and merge with the lowered continuum at the Mott density. Thus, an exciton gas is transformed into an electron-hole liquid. A highly sophisticated theory describing dynamical screening and degeneracy effects by the fermionic plasma constituents had been worked out, explaining precise measurements in excited semiconductors. However, because the ions are heavier compared to the effective mass of holes, a simple transfer of the physics of excited semiconductors to WDM is not possible. The ions remain classical within a large density region, forming strong correlations, which are described by the dynamical ionic structure factor (SF) $S_{\rm ii}(\mathbf{q},\omega)$.

*Corresponding author: chengliang.lin@uni-rostock.de
†gerd.roepke@uni-rostock.de
‡wolf-dietrich.kraeft@uni-rostock.de
§heidi.reinholz@uni-rostock.de

In the following, we will give a relation between the IPD and the ionic structure factor. Thus, mean-field (average atom) approaches are improved taking into account fluctuations of the ionic microfield. Further systematic improvements would be possible, considering higher order Feynman diagrams in the Green function approach.

II. THE IN-MEDIUM TWO-PARTICLE PROBLEM

We consider a two-particle system, consisting of an electron (charge $-e$, mass m_e) and an ion (charge $(Z_i+1)e$, mass m_i) embedded in a surrounding plasma. In vacuum, the solution of the Schrödinger equation for the Coulomb interaction is well known. Bound states are found at negative energies, whereas a continuum of scattering states is observed at positive energies. The simple case of the hydrogen atom can be generalized to a two-particle system with total charge $Z_i e$, consisting of a core ion with charge number Z_i+1 and an electron, charge number $Z_e=-1$. According to these definitions, the notations Z_i and Z_i+1 denote the charge number of the ions before and after the ionization, respectively. (Note that the charge number Z_i is at least by one smaller than the nuclear charge number of the corresponding atom. For neutral atoms before ionization, we have obviously $Z_i=0$.)

If the two-particle system is embedded in a plasma, bound-state energies and wave functions as well as the scattering states are modified. A systematic quantum statistical approach to describe these medium effects is given by the method of thermodynamic Green functions [20,26]. In particular, the following in-medium Schrödinger equation (or Bethe-Salpeter equation) can be derived [20,23,24,26]:

$$\Big[E(1)+E(2)+\sum_{\mathbf{q}}[f(1+\mathbf{q})+f(2-\mathbf{q})]V_{12}(\mathbf{q}) + \Delta V^{\rm eff}(1,2,\mathbf{q},z)\Big]\psi(1,2,z)+\sum_{\mathbf{q}}\{[1-f(1)-f(2)]V_{12}(\mathbf{q}) + \Delta V^{\rm eff}(1,2,\mathbf{q},z)\}\psi(1+\mathbf{q},2-\mathbf{q},z)=\hbar z\,\psi(1,2,z). \quad (1)$$

Here, the single particle states $1=\{\hbar\mathbf{p}_1,\sigma_1,c_1\}$ are given by momentum, spin, and species, respectively, $E(1)=\hbar^2\mathbf{p}_1^2/(2m_1)$. In the case considered here, c_1 and c_2 denote the electron and the core ion, respectively. For the interaction we assume the Coulomb potential $V_{12}(\mathbf{q})=Z_{c_1}Z_{c_2}e^2/(\varepsilon_0 q^2)$ which contains the charge numbers of the interacting particles, in our case $Z_{c_1}Z_{c_2}=-(Z_i+1)$.

The complex variable z describes the analytical continuation of the functions, defined for the Matsubara frequencies, into the entire z plane. Of interest is the behavior of the functions near the real axis, $z=\omega\pm i\epsilon$.

Neglecting in Eq. (1) the medium effects arising from the effective interaction $\Delta V^{\rm eff}(1,2,\mathbf{q},z)$ as well as the Fermi distribution functions $f(i)=\{\exp\beta[E(i)-\mu(i)]+1\}^{-1}$ with $\beta=1/(k_BT)$ and $\mu(1)$ denoting the chemical potential of species c_1, the equation

$$[E(1)+E(2)]\psi(1,2,z)+\sum_{\mathbf{q}}V_{12}(\mathbf{q})\psi(1+\mathbf{q},2-\mathbf{q},z) = \hbar z\,\psi(1,2,z) \quad (2)$$

has eigensolutions $\psi_n(1,2)$ at energies $\hbar z=E_n$, well known from hydrogen-like ions. For more complex ions consisting of a nucleus and some bound electrons, a pseudopotential can be introduced to describe the effect of the electrons within the core ion.

The in-medium Schrödinger Eq. (1) describes the influence of the medium by two effects, Pauli blocking and screening. Pauli blocking is caused by the antisymmetrization of the fermionic wave function. States which already are occupied by the medium are blocked and can not be used for the two-particle system under consideration. The blocking is described by the Fermi distribution function. Pauli exclusion principle is acting as Fock shift $\sum_{\mathbf{q}} f(1+\mathbf{q})\,V_{12}(\mathbf{q})$ in addition to the single particle energy $E(1)$ in Eq. (1) (for charge-neutral plasmas, the Hartree term vanishes). Also in the interaction term, Pauli blocking gives the contribution $-\sum_{\mathbf{q}} f(1)V_{12}(\mathbf{q})\psi(1+\mathbf{q},2-\mathbf{q},z)$. Both in-medium contributions are caused by the degeneracy of the plasma particles. In the plasmas considered here, electrons may be degenerate because of their small mass m_e. The ions are nondegenerate and can be treated as classical particles.

Considering only the Pauli blocking effects, the effective (non-Hermitean) Hamiltonian of Eq. (1) remains real and can be symmetrized. The energy eigenvalue problem can be solved, and the bound-state energies as well as the edge of continuum states are shifted. At a certain density, the bound states merge with the continuum of scattering states and disappear. Within this approximation, which is essentially a mean-field approximation, a sharp value for the lowering of the continuum edge and for the IPD can be calculated.

Screening of the interaction by the medium is described by the effective interaction

$$\Delta V^{\rm eff}(1,2,\mathbf{q},z) = -V_{12}(\mathbf{q})\int_{-\infty}^{\infty}\frac{d\omega'}{\pi}\,{\rm Im}\,\varepsilon^{-1}(q,\omega'+i0) \times[n_{\rm B}(\omega')+1]\left[\frac{\hbar}{\hbar z-\hbar\omega'-E(1)-E(2-\mathbf{q})} + \frac{\hbar}{\hbar z-\hbar\omega'-E(1+\mathbf{q})-E(2)}\right], \quad (3)$$

where terms $\propto f(1)$, which give corrections in higher orders of the density, are neglected. $n_{\rm B}(\omega)=[\exp(\beta\hbar\omega)-1]^{-1}$ is the Bose distribution function. The dynamical properties of the surrounding plasma are contained in the dielectric function $\varepsilon(q,z)$ to be taken at the real axis, $z=\omega'+i0$. In general, this is a complex, frequency-dependent quantity, with a jump of the imaginary part at the real axis. Often the random-phase approximation (RPA) is taken, and in the static limit $\omega\to 0$ the Debye screening is obtained. In this work, we show that these simple approximations have to be improved in a systematic way, which is obtained from the quantum statistical approach.

Including the effective potential, the effective Hamiltonian in the in-medium Schrödinger Eq. (1) becomes complex and frequency dependent. As a consequence, the eigenstates are no longer stationary states with sharp energy levels that are shifted by the polarization of the medium, but have a finite lifetime given by the imaginary part of the effective Hamiltonian. This can be interpreted as collisions with the plasma particles and

leads to a broadening of the energy levels. The corresponding quantum statistical approach to plasma line shapes based on the treatment of the polarization function has been worked out [21] and will not be investigated in the present work.

Subsequently, sharp level shifts and a sharp shift of the continuum edge are only obtained from a mean-field approximation. Any frequency dependence beyond the mean-field approximation gives imaginary parts and, in this way, a broadening of the continuum edge and the energy levels. The latter problem has been considered also earlier [22,24], where both real part and imaginary part of the energy levels of the in-medium two-particle problem are calculated. As a consequence, only the spectral function has a unique physical meaning, showing the spectral line profiles and the smooth transition to the continuum. However, within this work we will focus on the shifts that are obtained from the real part of the effective Hamiltonian.

As shown in Refs. [20,22–24,26], density effects arise from dynamical screening in the effective potential, expressed by the inverse dielectric function $\varepsilon^{-1}(q,z)$ of the medium in Eq. (3). For bound states, Pauli blocking as well as the screening in the self-energy term [$\Delta V^{\rm eff}$ in the first square bracket of Eq. (1)] and the effective interaction partially compensate each other so that the bound-state energy levels are only weakly dependent on the density. In contrast, the energy shift of the continuum states is determined only by the self-energy contribution. Therefore, in leading order of the density, the medium modification of the IPD is given by the shift of the edge of continuum states. For a more extended discussion, see Refs. [20,22–26].

A standard expression for the dielectric function $\varepsilon(q,z)$ is the random phase approximation (RPA). From the real part of the self-energy, the Debye shift of the continuum edge is immediately observed. Here we discuss improvements beyond RPA to evaluate the shift of the continuum edge occurring at $\mathbf{p}_1 = \mathbf{p}_2 = 0$. Thus, our approach, which is based on a systematic quantum statistical approach, can be regarded as an improvement of the Debye theory or other approaches using semiempirical assumptions such as the ion sphere model.

III. SHIFT OF SINGLE-PARTICLE STATES

A. Self-energy of single-particle states

In the single-particle picture, the influence of the plasma environment on the properties of the investigated particle is merged into the self-energy $\Sigma_c(1,z)$. It can be represented by Feynman diagrams, in lowest approximation by the diagram (also known as V^sG or GW approximation) with the dressed propagator G and the screened potential V^s,

$$\Sigma_c(1,z) = \sum_{\mathbf{q},\omega} G_c(\mathbf{p}-\mathbf{q}, z-\omega)\cdot V^s(\mathbf{q},\omega)$$

$$= \quad = \Sigma_c^{\rm HF}(1,z) + \Sigma_c^{\rm corr}(1,z). \qquad (4)$$

The Hartree-Fock (HF) contribution to the self-energy has been investigated elsewhere, see Ref. [20], and will not be discussed here. The correlation part of the self-energy $\Sigma_c^{\rm corr}(1,z)$ contains the contribution of the interaction with electrons, as well as the interaction with ions. We are interested in the real part of the self-energy since it describes the continuum shift. It follows from Eq. (3) by renaming, e.g., $\hbar z - E(2) = \hbar\omega$ in the last term of Eq. (3). Then we have

$$\mathrm{Re}\,\Sigma_c^{\rm corr}(p,\omega) = -\mathcal{P}\int \frac{d^3\mathbf{q}}{(2\pi)^3}\int\frac{d\omega'}{\pi} V_{cc}(q)\,\mathrm{Im}\,\varepsilon^{-1}(q,\omega'+i0)\frac{1+n_{\rm B}(\omega')}{\omega-\omega'-E_{c,\mathbf{p}+\mathbf{q}}/\hbar}. \qquad (5)$$

($\mathcal{P}$ denotes the principal value.) In general, the dielectric function is connected to the dynamical SF via the fluctuation-dissipation theorem. For a two-component plasma (free electrons with charge $-e$, ions with effective charge Z_ie and charge neutrality $Z_in_i = n_e$), the imaginary part of the inverse dielectric function can be expressed via the dynamical SFs, see also Ref. [27],

$$\mathrm{Im}\,\varepsilon^{-1}(\mathbf{q},\omega+i0) = \frac{e^2}{\varepsilon_0 q^2}\frac{\pi}{\hbar\,(1+n_{\rm B}(\omega))}\left[Z_i^2\, n_i\, S_{\rm ii}(\mathbf{q},\omega) - 2Z_i\sqrt{n_e n_i}\,S_{\rm ei}(\mathbf{q},\omega) + n_e S_{\rm ee}(\mathbf{q},\omega)\right]. \qquad (6)$$

The dynamical SFs $S_{cd}(\mathbf{q},\omega)$ characterize the plasma in response to any perturbation. For instance, they have been investigated to describe x-ray Thomson scattering; see Ref. [28]. Other plasma properties, such as the electrical conductivity, are also governed by the dynamical SF. The dynamical SFs are related to the density-density correlation functions $\langle\delta n_c(\mathbf{r},t)\delta n_d(0,0)\rangle$ via Fourier transformation. Note, that it is also connected to the symmetrized correlation function of the longitudinal microfield fluctuations $\langle\delta\mathbf{E}\delta\mathbf{E}\rangle_{\mathbf{q},\omega}$ [26],

$$\langle\delta\mathbf{E}\delta\mathbf{E}\rangle_{\mathbf{q},\omega} = 2\pi\left(Z_i^2e^2/q^2\right)S_{\rm ii}(\mathbf{q},\omega). \qquad (7)$$

For further discussion of the general expressions Eqs. (5) and (6), we perform exploratory calculations using model approaches for the dynamical SFs. Following the relations for the dynamical SFs reported in Refs. [27,28],

$$S_{\rm ei}(q,\omega) = \frac{q_{\rm sc}(k)}{\sqrt{Z_i}}S_{\rm ii}(q,\omega),$$

$$S_{\rm ee}(q,\omega) = S_{\rm ee}^0(q,\omega) + \frac{|q_{\rm sc}(k)|^2}{Z_i}S_{\rm ii}(q,\omega), \qquad (8)$$

the decomposition of the dynamical SF as introduced in Eq. (6) can be divided into $S_{\rm ee}^0(q,\omega)$ of the fast moving free electrons and the ionic part $S_{\rm ii}^{ZZ}(q,\omega)$, which includes also the screening cloud of the slowly moving electrons following the ionic motion, denoted by $q_{\rm sc}(k)$,

$$Z_iS_{\rm ii}(q,\omega) - 2\sqrt{Z_i}S_{\rm ei}(q,\omega) + S_{\rm ee}(q,\omega)$$
$$= Z_i\,S_{\rm ii}^{ZZ}(q,\omega) + S_{\rm ee}^0(q,\omega), \qquad (9)$$

with $S_{\rm ii}^{ZZ}(q,\omega) = (1 - q_{\rm sc}(k)/Z_i)^2 S_{\rm ii}(q,\omega)$. The electronic contribution to the continuum lowering is described by the electronic SF $S_{\rm ee}^0$ and has been widely discussed; see Refs. [20,26]. Results in the Montroll-Ward approximation are well known. Compared to the ionic contribution ($\sim Z_i^2 e^2$), the electronic contribution ($\sim e^2$) is usually quite small for highly charged states.

Following Eqs. (5) and (6), we now discuss the ionic contribution to the correlation shift of the continuum edge $\mathrm{Re}\,\Sigma_e^{\rm corr}(0,\omega) + \mathrm{Re}\,\Sigma_i^{\rm corr}(0,\omega)$. It is expressed as

$$\begin{aligned}\mathrm{Re}\,\Sigma_c^{\rm corr,\,ion}(p=0,\omega) &= \Delta_c^{\rm ion}(0,\omega)\\ &= -\mathcal{P}\int\frac{d^3\mathbf{q}}{(2\pi)^3}\int\frac{d\omega'}{\pi}\frac{V_{cc}(q)}{\omega-\omega'-E_{c,\mathbf{q}}/\hbar}\\ &\quad\times\frac{\pi Z_i e^2 n_e}{\hbar\epsilon_0 q^2}S_{\rm ii}^{ZZ}(q,\omega'). \qquad (10)\end{aligned}$$

Thus, the ionic contribution to the continuum shift is related to the dynamical SF of the ions. The quasiparticle shift has to be defined self-consistently at $\omega = \Delta_c^{\rm ion}(0,\omega)$, but this shift is compensated in the denominator of the integrand by the energy $E_{c,\mathbf{q}}$, which is shifted too. Then the ionic contribution $\Delta_c^{\rm ion}(0,\omega)$ is given by $\Delta_c^{\rm ion}(0,0)$, later denoted as $\Delta_c^{\rm ion}$.

B. Plasmon pole approximation

Under WDM conditions considered here, the ions are strongly coupled, so that the SF $S_{\rm ii}^{ZZ}$ should not be taken in the Debye limit. However, the plasma ions can be treated classically. Therefore, for $\Delta_c^{\rm ion}(0,0)$, see Eq. (10), we consider the limit $\hbar \to 0$ in the propagator $1/[-\omega' - \hbar q^2/(2m_c)]$. In addition, the ions move very slowly in comparison to the electrons, which indicates that it is reasonable to replace the dynamical SF of ions by the static SF within some approximations. We use the plasmon pole approximation $\mathrm{Im}\,\varepsilon_{\rm ion}^{-1}(q,\omega) = -\pi\omega_i^2\{\delta(\omega-\omega_{q,i}) - \delta(\omega+\omega_{q,i})\}/(2\omega_{q,i})$, where $\omega_{q,i}^2 = (q^2\omega_i^2)/(\kappa_i^2 S_{\rm ii}^{ZZ}(q))$ is fulfilling the f-sum rule [28] with the ionic plasmon frequency $\omega_i^2 = Z_i^2 n_i e^2/(\epsilon_0 m_i)$ and the inverse Debye screening parameter $\kappa_i^2 = \omega_i^2 m_i/k_B T$. Then we find the following expression:

$$S_{\rm ii}^{ZZ}(q,\omega) \approx S_{\rm ii}^{ZZ}(q)\,\frac{\delta(\omega-\omega_{q,i}) + \delta(\omega+\omega_{q,i})}{1+e^{-\hbar\omega/(k_B T)}}. \qquad (11)$$

The physical meaning of the replacement of the dynamical SF by the static SF in Eq. (11) is that the ions are considered to have a fixed distribution in the plasma neglecting temporal fluctuations.

For the ionization process $i_{Z_i} \to e + i_{Z_i+1}$, the IPD can be given by the difference between the self-energy before and after the ionization of the investigated system; i.e., $\Delta_{\rm IPD}^{\rm ion} = \Delta_i^{\rm ion} - (\Delta_e^{\rm ion} + \Delta_{i+1}^{\rm ion})$. We assume that the ionic structure of the plasma environment does not change during the ionization. Therefore, we insert Eq. (11) into $\Delta_c^{\rm ion}$; see Eq. (10). Performing the approximations as discussed in context with Eq. (10), we obtain for the IPD,

$$\Delta_{\rm IPD}^{\rm ion} = -\frac{(Z_i+1)e^2}{2\pi^2\epsilon_0}\frac{\kappa_i^2}{k_{{\rm F},i}}\int_0^\infty\frac{dq_0}{q_0^2}S_{\rm ii}^{ZZ}(q_0), \qquad (12)$$

where $q_0 = q/k_{{\rm F},i}$ is the reduced wave number with $k_{{\rm F},i} = (3\pi^2 n_i)^{1/3}$. Considering the ion-ion SF $S_{\rm ii}^{\rm DH}(q) = q^2/(q^2+\kappa_i^2)$ of a one-component plasma (OCP), valid in the low density and the high temperature limits, the DH result $\Delta_{\rm DH}^{\rm ion} = -(Z_i+1)e^2\kappa_i/(4\pi\varepsilon_0)$ is recovered for the ionic contribution to the IPD. Equation (12) shows a strong dependence on the temperature indicated by the inverse Debye length κ_i appearing in the frequency $\omega_{q,i} \sim \kappa_i^{-1}$ in Eq. (11), and also by the static ionic SF. The screening parameter $\kappa_i^2 \propto 1/(k_B T)$ follows from the linearized Debye theory for classical systems. Nevertheless, with increasing coupling parameter, the plasma starts to crystallize and forms a periodic structure. In this case, the frequency $\omega_{q,i}$ is determined by the Wigner-Seitz radius $r_{\rm ws} = (4\pi n_i/3)^{-1/3}$, as discussed, e.g., in Ref. [29]. Consequently, the parameter κ_i^2 occuring in $\omega_{q,i}$ should be replaced by a more general expression $\tilde{\kappa}_i^2(\Gamma_i)$ depending on the ionic coupling parameter $\Gamma_i = Z_i^2 e^2/(4\pi\epsilon_0 k_B T r_{\rm ws})$. We can express Eq. (12) in the form

$$\Delta_{\rm IPD}^{\rm ion} = -\frac{(Z_i+1)e^2}{2\pi^2\epsilon_0 r_{\rm ws}}S(\Gamma_i), \qquad (13)$$

introducing the parameter function

$$S(\Gamma_i) = F(\Gamma_i)\int_0^\infty\frac{dq_0}{q_0^2}S_{\rm ii}^{ZZ}(q_0). \qquad (14)$$

From the Debye-Hückel theory follows

$$F(\Gamma_i) = \frac{\kappa_i^2 r_{\rm ws}}{k_{{\rm F},i}} = \left(\frac{4}{9\pi}\right)^{1/3} r_{\rm ws}^2\,\kappa_i^2 = \Gamma_i\left(\frac{12}{\pi}\right)^{1/3}, \qquad (15)$$

valid for weakly coupled system $\Gamma_i \ll 1$. For strong coupling, a similar type of expression, $F(\Gamma_i) = \sqrt[3]{4/(9\pi)}r_{\rm ws}^2\,\tilde{\kappa}_i^2(\Gamma_i)$ can be defined and will be discussed in detail in the next section. One should keep in mind that, for a fixed charge state Z_i, the parameter function $S(\Gamma_i)$ should gradually tend to a constant due to crystallization of the plasma with increasing coupling parameter [29]. At a fixed temperature and density, the parameter function $S(\Gamma_i)$ slightly depends on the charge number since the dependence on charge number Z_i in the static ionic SF $S_{\rm ii}^{ZZ}(q_0)$ compensates with that of the function $F(\Gamma_i)$.

The approach presented in this work shows a close connection of the IPD to the detailed structure of the plasma system. The general expression Eq. (13) with Eq. (14) should work within the valid range of the fluctuation-dissipation theorem for both equilibrium and non-equilibrium systems described by the static SF of the quantum many-body system. Once the SF is known from other methods, for instance, simulations or Thomson scattering measurements, the IPD can be directly evaluated. In this work, the local thermodynamic equilibrium is assumed for the calculation. Further investigations are needed to describe nonequilibrium situations, for instance, after irradiations by strong short-pulse laser beams.

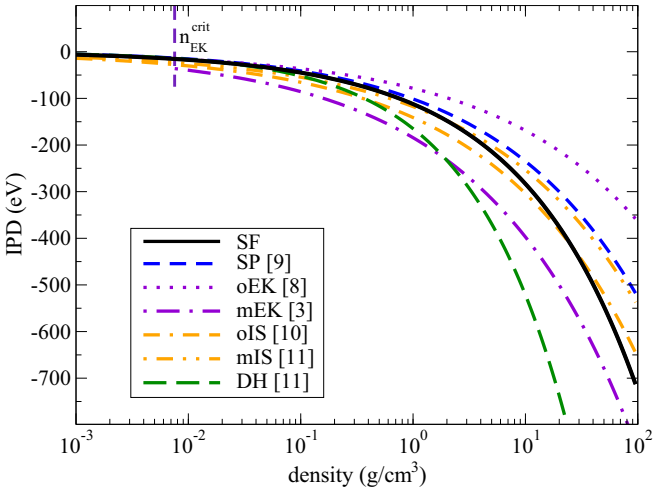

FIG. 1. IPD for Al^{11+} at 600 eV as function of the density, calculated using our model (SF) and by different theoretical models.

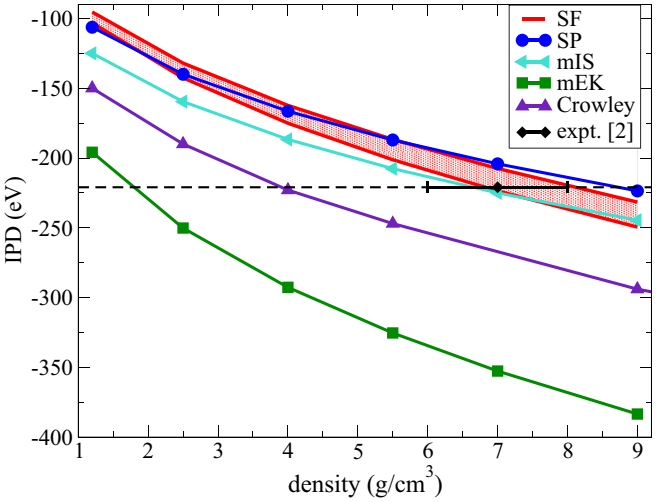

FIG. 2. IPD for Al^{11+} in aluminum plasma at 600 eV for the density as relevant for the experiment [2], calculated by different theoretical models, i.e., SP [9], mEK [3], and mIS as well as Crowley's calculation [11]. The horizontal line indicates the unperturbed ionization potential of the upper level of the Al^{11+} He_β line [30]. The full line (diamond with error bar) marks the critical density range observed experimentally [2]. The (red) shaded area shows the result from our model (SF) for temperatures in the range of 550 to 700 eV.

IV. RESULTS AND DISCUSSION

A. Model calculation: comparison to other approaches

To determine the function $F(\Gamma_i)$ in the parameter function $S(\Gamma_i)$, Eq. (14), the implicit normalization relation [20],

$$\int_0^\infty dx x^2 \left\{1 - \exp\left[-\frac{\Gamma_i}{x}\exp(-\tilde{\kappa}_i(\Gamma_i) r_{ws}\, x)\right]\right\} = \frac{1}{3}, \qquad (16)$$

according to the nonlinear Debye theory is used, which avoids negative densities of the screening cloud. The Debye-Hückel theory can be recovered by expanding the exponential function outside of the square brackets up to the first order in Γ_i; see Eq. (15). For intermediate and strong coupling, Eq. (16) has to be solved numerically. In this work, we introduce the following expression:

$$F(\Gamma_i) = \sqrt[3]{\frac{4}{9\pi}} r_{ws}^2\, \tilde{\kappa}_i^2(\Gamma_i) = \frac{3\Gamma_i}{\sqrt{(9\pi/4)^{2/3} + 3\Gamma_i}}, \qquad (17)$$

as an approximation that reproduces the Debye-Hückel limit Eq. (15) as well as the numerical solutions of Eq. (16) in the strong coupling regime of interest.

In general, the pair correlation function exhibits a peak near r_{ws} when approaching the liquid state, which would be reasonably well described by a Percus-Yevick SF. In the intermediate density region, an interpolation formula for the ionic SF can be applied; see Ref. [28]. In the following, we use Eq. (13) together with Eq. (17) and the static ionic SF as given in Ref. [28] to evaluate the ionic contribution to the IPD in the plasma.

As an exploratory calculation to compare to other theoretical models, we consider the IPD of the ion Al^{11+} ($Z_i = 11$) at a temperature of 600 eV. Figure 1 shows the IPD calculated using different theoretical models. It can been seen, that the IPD from SP [9], original EK (oEK) [8] and our result are in good agreement with the DH shift in the low-density region. Above the critical density $n_{EK}^{crit} = 3/(4\pi)[4\pi\varepsilon_0 k_B T/(Z^2 e^2)]^3$ with the nuclear charge Ze, the underestimation of the IPD by the SP model and the overestimation by the modified EK (mEK) model [3] can be seen in comparison to the original IS (oIS) model. Note that, with increasing density, corresponding to increasing coupling parameter Γ_i ($\Gamma_i = 0.16$ for the density 0.001 g/cm^3 and $\Gamma_i = 7.28$ for the density 100 g/cm^3), our result shows, on one hand, a transition from SP at low densities (weakly and moderately coupled) to mEK at large densities (strongly coupled), and, on the other hand, a good agreement with the oIS model in the intermediate density region.

B. Numerical results for experimental conditions

We now discuss the application of our model calculation to conditions observed in experiments. In the experiments of Hoarty *et al.* [2,16], the spectral lines emitted from Al^{11+} were observed. The investigated density range is 1.2 to 9 g/cm^3 at electron temperatures in the range of 550 to 700 eV. The disappearance of the He_β line would be due to the dissolution of $n = 3$ levels. The assumption of local thermodynamic equilibrium is believed to be valid for the high densities [16], which implies the ionic coupling parameter is estimated to be in the range of 2–4. In such a moderate coupling regime, the SP and IS models should result in the best agreement with the experiment, as can be seen by looking at the relevant density range in Fig. 1.

The latter is shown in Fig. 2 for a more detailed discussion. The horizontal line denotes the unperturbed ionization potential (220 eV) of the upper level of the Al^{11+} He_β line [30]. The density range, in which the disappearance of Ly_β and He_β lines in aluminum plasma [2] was measured, is marked as solid line. It occurs at a density somewhere between 5.5 and 9 g/cm^3, which is in reasonable agreement with the predictions by FLYCHK [1] using the SP model. According to calculations based on a generalized ion-cell model by Crowley [11], for this range of densities, the modified IS (mIS) model is most suitable. This is consistent with predictions for spectra using the CASSANDRA opacity code with an IS model for the

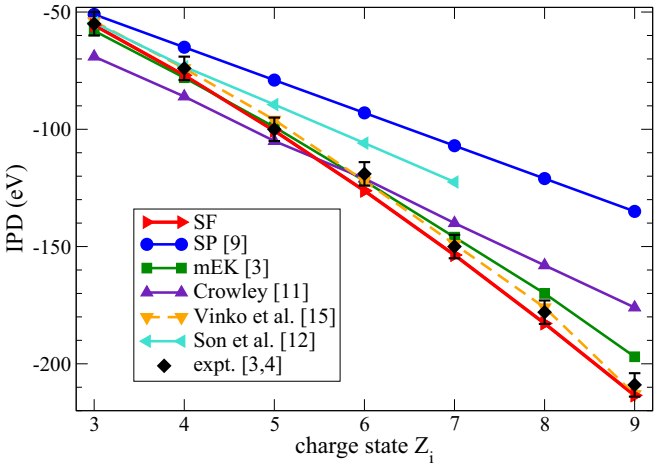

FIG. 3. IPD for aluminum plasma at solid density 2.7 g/cm^3 as function of different charge states. Shown are experimental results [3,4] in comparison to our model (SF) and other theoretical models. (Lines to guide the eye.)

IPD [16], where the dissolution of lines from $n = 3$ levels is indicated to take place between the density of $6 \sim 8$ g/cm^3. As shown in Fig. 2, the EK model results in much larger IPD values in comparison to the SP model, and hence leads to a disappearance of spectral lines at a lower density of about 2 g/cm^3. A similar estimate was given in the calculation by Crowley [11]. Our approach, predicting a critical density between $7 \sim 8$ g/cm^3 for the disappearance of $n = 3$ levels, gives also an excellent agreement with the experimental data and with the predictions by the CASSANDRA opacity code [16].

Using FEL [3,4], further experiments have been performed recently. An aluminum sample at solid density was isochorically heated up to electron temperatures of 200 eV, indicating a strongly coupled plasma, and the IPD was directly measured for different charge states. The LCLS pulse duration in this experiment was estimated to be less than 80 fs. The ionic plasma frequency $\omega_{\rm pl}^{\rm ion}$ in this laser-produced plasma is found to be in the order of 10^{14}/s. In contrast, the response of the electrons to the laser field is much faster and can be described by the electron frequency $\omega_{\rm pl}^{\rm el} \sim 10^{16}$/s. In comparison to the laser pulse, the electrons have enough time to exchange energy between each other and with the laser field and are isochorically heated to a high temperature. Because of the large mass of the ions, the response of the ionic subsystem to the external fluctuations is so slow that the ions in the plasma are weakly excited by the photons and by fast moving electrons, which implies that the ions are colder than the electrons. Of essential importance in the measurement is that the IPD for distinct charge states, inferred from the triggering energy of the photoionization, is measured at different time stages. This fact indicates that the ions are heated during the time evolution and local thermal equilibrium may be achieved.

Figure 3 shows the experimental results in comparison to several calculations using different theoretical models. The direct measurement of the IPD in aluminum plasma can be explained reasonably well by the mEK model as discussed in Ref. [3]. Vinko *et al.* [15] performed detailed calculations on electronic structures of Al ions in a plasma via the finite-temperature DFT method. They found that the IPD for a given charge state could be well understood in terms of the electronic structure of valence electron states near core-excited ions within a pseudoneutral atom approximation. The results from the two-step Hartree-Fock calculations by Son *et al.* [12] and from the calculations by Crowley [11] are less satisfying. However, as shown in Fig. 3, the experimental data can also be reproduced by our approach, where the effect of the surrounding plasma on the ions is directly accounted for by the screened ionic SF. In our calculation, the LTE condition was assumed. This might not be suitable for the experimental measurements where the ions remain relatively cold because of the femtosecond nature of the x-ray pulse [15]. For this nonequilibrium case, the ionic SF under non-LTE conditions should be taken into account. However, detailed calculations of the ionic SF in the non-LTE case are rather intricate and are still in progress.

TABLE I. IPD in eV and mean charge for CH mixture at density 6.74 g/cm^3 and $T = 86$ eV [7]. The ionization energies for different charge states are $I[C^{3+}] = 64.5$ eV, $I[C^{4+}] = 392.1$ eV, $I[C^{5+}] = 490.0$ eV. We have taken in our calculation an effective SF, where x is the carbon ratio. (For Refs. see Fig. 1.)

Model \ Charge	C^{3+}	C^{4+}	C^{5+}	Mean charge
DH	261.3	326.7	392.0	4.91
SP	91.7	108.3	123.9	4.18
IS	103.2	119.7	135.2	4.21
mEK	116.0	145.0	174.0	4.24
SF ($x = 0.75$)	237.3	296.6	355.9	4.79
SF ($x = 1$)	99.0	123.7	148.4	4.19
Expt.				4.92 ± 0.15

The application of simple IPD models (e.g., SP) to a mixture of different ions is problematic as displayed by recent measurements on a CH mixture at NIF [7]. The obtained mean charge state can not be explained by either the SP or the mEK models, as shown in Table I. Although the DH shift is inappropriate under the experimental conditions [strong coupling of the carbon ions ($\Gamma_{\rm C} \sim 4$)], it results in larger IPDs and therefore gives a more reasonable agreement with the experiment than all other models. This fact can be attributed to the deficiency to account for strong correlation and fluctuation effects in these models.

For the CH mixture, the influence of a different chemical species, the protons from the fully ionized hydrogen, on the properties of the carbon ions is, within SP and EK models, described by an additional electron density. In our approach, this effect can be more consistently taken into account by the ionic SF, which includes the response of all charged particles in the plasma. We applied the linear mixing rule [31] for the SF of a multicomponent plasma, $S_{\rm ii}^{\rm ZZ}(q_0) = x\, S_{\rm CC}^{\rm ZZ}(q_0) + (1-x)\, S_{\rm HH}^{\rm DH}(q_0)$. For the ratio $x = 0.75$ of carbon, an estimated mean charge of 4.79 and therefore a close match with the experimental value of 4.92 ± 0.15 [7] is found. Under the experimental conditions [7], the carbon ions are strongly coupled while the protons are weakly correlated. The SF of the protons modifies the structure of the integrand in Eq. (14) leading to higher IPD values for the carbon ions, and therefore push the carbon ions to a higher charge state.

Calculations for a pure C plasma at the same conditions (same ionic density of carbon and same temperature), lead to the mean ionization degree of 4.2. For the CH plasma, the asymmetry of the charges and masses of protons and carbon ions lead to strong fluctuations and hence significantly enhance the ionization. Future discussions on experiments with pure C targets may test this effect.

More recently, a new experimental study on the ionization states of warm dense aluminum ($T_e \sim 20$–25 eV and $\rho \sim 2.7$ g/cm^3) was performed [32]. It was found that the observed time-dependent absorption spectra are better described using the mEK model for the IPD than using SP and IS models. This result agrees with our findings. For the given experimental conditions, the ion charge states Al^{4+} and Al^{5+} are clearly seen, which indicates an ion coupling parameter of $\Gamma_i \sim 7$. As discussed for Fig. 1, in such strongly coupled systems, the mEK model should lead to a better description for the IPD.

V. CONCLUSIONS AND FURTHER IMPROVEMENTS

We treated the in-medium two-particle problem Eq. (1) within a quasiparticle approach and obtained the contribution of the shift of the continuum edge to the IPD. In addition to the continuum edge, also the bound-state energy levels are shifted. Although their shifts are small as compared to the continuum lowering, see Refs. [20,22–24,26], these bound-state level shifts should also be considered in a detailed calculation for the IPD. Note that the shift of bound-state levels has been observed in the shift of spectral lines, and quantum statistical calculations [21] agree well with experimental data.

A more serious problem is the use of the quasiparticle approximation. Within a sophisticated Green function approach, the quasiparticle propagators are replaced by spectral functions, see, e.g., Ref. [33], which describe also the finite life time of the quasiparticle excitations. This leads to the fact that the energy gaps between the optical lines describing bound-state transitions are washed out (Inglis-Teller effect [34]).

In his monograph, Griem [35] described the broadening of spectral lines by the Stark effect leading to a shift of the observed series limit. The latter is described by

$$n_s^{z-1} = \tfrac{1}{2} z^{3/5} \left(a_0^3 N_e\right)^{-2/15}, \tag{18}$$

with n_s the main quantum number and N_e the electron number density. Equation (18) was determined by a fit to a Holtsmark profile [36] and corresponds to Eq. (4) in Ref. [34]. Griem mentions that the shift of the series limit where lines fully overlap does not have a direct relation to the lowering of the ionization potential (last paragraph of Sec. 5.7 in Ref. [35]). As discussed in Sec. II, definite values for the plasma parameters, where the ionization potential vanishes, can only be given within a quasiparticle (mean field) approximation which gives sharp energy levels. As soon as the imaginary part of the effective Hamiltonian Eq. (3) is taken into account, the sharp energy levels become broadened as a consequence of their finite life time owing to collisions with the plasma particles. Consequently, the rigorous discrimination between bound states (having a finite life time) and continuum states (including resonances) is no longer possible, and, strictly speaking, the concept of IPD based on sharp quasiparticle energy levels becomes obsolete.

We performed exploratory calculations using a simple model for the dynamical SF Eq. (11). As a main result, we found that correlations that are described by the ionic SF are indeed relevant for the IPD. As proposed, it would be of interest to perform experiments with pure substances like C. Compared to the large IPD seen in CH experiments [7], a lower IPD is expected for a pure C plasma. More details of the ionic subsystem may be incorporated, in particular, the relaxation of the ionic subsystem and collective excitations (plasmons, phonons) can be treated. For a discussion, see also Ref. [11].

Our approach is based on a Born approximation for the interaction of the two-particle system with the plasma ions. The internal structure and dynamics of the plasma is described by the dielectric function which contains the polarization function $\Pi(\mathbf{q},\omega)$,

$$\varepsilon(\mathbf{q},\omega) = 1 - \frac{1}{\epsilon_0 q^2} \Pi(\mathbf{q},\omega). \tag{19}$$

Improving the RPA expression for the polarization function, two-particle correlations are included, see also [37]. In particular, the ionic dynamical structure factor is taken into account if the cluster decomposition of the polarization function is considered, here the two-ion distribution. Similar approaches have been used for the optical spectra [21] where also a cluster decomposition of the polarization function has been considered.

This discussion gives a conception of how to improve our approach. The Born approximation has to be completed accounting for multiple interaction (so-called T matrix). A more general diagram for the self-energy looks like

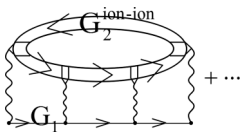

where the double line denotes the two-ion propagator, and the screened interaction with the investigated particle is considered in ladder approximation. The approximation Eq. (4) for the self-energy results from the first contribution of the ladder sum which contains only two electron-ion interaction lines.

Starting from the general expression Eq. (4), we obtain a rather simple formula Eq. (13) for the IPD containing the ionic static structure factor. We emphasize that this result could now be improved by systematically removing again some of the approximations for the dynamical SF Eq. (11). In particular, the plasmon pole approximation in handling the dynamical SF is a model assumption which can be improved, e.g., by numerical simulations. Finally, an advantage of our quantum statistical approach is that any degeneracy effect can be taken into account in a systematic way, which becomes of interest at increasing densities.

ACKNOWLEDGMENTS

One of the authors (C.L.) thanks S. Vinko for making experimental data available and D. Kraus, D. Hoarty, and Y. Hou for helpful discussions. This work is supported by the German Research Foundation DFG within SFB Grant No. 652.

[1] H.-K. Chung *et al.*, High Energy Density Phys. **1**, 3 (2005).
[2] D. J. Hoarty *et al.*, Phys. Rev. Lett. **110**, 265003 (2013).
[3] O. Ciricosta *et al.*, Phys. Rev. Lett. **109**, 065002 (2012).
[4] O. Ciricosta *et al.*, Nat. Commun. **7**, 11713 (2016).
[5] T. R. Preston *et al.*, High Energy Density Phys. **9**, 258 (2013).
[6] L. B. Fletcher *et al.*, Phys. Rev. Lett. **112**, 145004 (2014).
[7] D. Kraus *et al.*, Phys. Rev. E **94**, 011202(R) (2016).
[8] G. Ecker and W. Kröll, Phys. Fluids **6**, 62 (1963).
[9] J. C. Stewart and K. D. Pyatt, Jr., Astrophys. J. **144**, 1203 (1966).
[10] G. Zimmerman and R. More, J. Quant. Spectrosc. Radiat. Transfer **23**, 517 (1980).
[11] B. J. B. Crowley, High Energy Density Phys. **13**, 84 (2014).
[12] S.-K. Son, R. Thiele, Z. Jurek, B. Ziaja, and R. Santra, Phys. Rev. X **4**, 031004 (2014).
[13] M. Stransky, Phys. Plasmas **23**, 012708 (2016).
[14] A. Calisti, S. Ferri, and B. Talin, Contrib. Plasma Phys. **55**, 360 (2015); J. Phys. B **48**, 224003 (2015).
[15] S. M. Vinko, O. Ciricosta, and J. S. Wark, Nat. Commun. **5**, 3533 (2014).
[16] D. J. Hoarty *et al.*, High Energy Density Phys. **9**, 661 (2013).
[17] C. A. Iglesias and P. A. Sterne, High Energy Density Phys. **9**, 103 (2013).
[18] C. A. Iglesias, High Energy Density Phys. **12**, 5 (2014).
[19] M. W. C. Dharma-wardana and F. Perrot, Phys. Rev. A **45**, 5883 (1992).
[20] W.-D. Kraeft, D. Kremp, W. Ebeling, and G. Röpke, *Quantum Statistics of Charged Particle Systems* (Akademie-Verlag, Berlin, and Plenum Press, London/New York, 1986).
[21] S. Günter, L. Hitzschke, and G. Röpke, Phys. Rev. A **44**, 6834 (1991).
[22] J. Seidel, S. Arndt, and W.-D. Kraeft, Phys. Rev. E **52**, 5387 (1995).
[23] G. Röpke, K. Kilimann, D. Kremp, W. D. Kraeft, and R. Zimmermann, Phys. Status Solidi B **88**, K59 (1978).
[24] R. Zimmermann, K. Kilimann, W. D. Kraeft, D. Kremp, and G. Röpke, Phys. Status Solidi B **90**, 175 (1978).
[25] R. Zimmermann, *Many-Particle Theory of Highly Excited Semiconductors* (Teubner, Leipzig, 1987).
[26] D. Kremp, M. Schlanges, W.-D. Kraeft, and T. Bornath, *Quantum Statistics of Nonideal Plasmas* (Springer-Verlag, Berlin/Heidelberg, 2005).
[27] J. Chihara, J. Phys.: Condens. Matter **12**, 231 (2000).
[28] G. Gregori, A. Ravasio, A. Höll, S. H. Glenzer, and S. J. Rose, High Energy Density Phys. **3**, 99 (2007).
[29] G. Kalman and K. I. Golden, Phys. Rev. A **41**, 5516 (1990).
[30] A. Kramida, Y. Ralchenko, J. Reader, and NIST ASD Team (2015), *NIST Atomic Spectra Database* (ver. 5.3, online).
[31] J. Daligault and S. Gupta, Astrophys. J. **703**, 994 (2009).
[32] M. Z. Mo *et al.*, Phys. Rev. E **95**, 053208 (2017).
[33] C. Fortmann, Phys. Rev. E **79**, 016404 (2009).
[34] D. R. Inglis and E. Teller, Astrophys. J. **90**, 439 (1939).
[35] H. R. Griem, *Plasma Spectroscopy* (McGraw-Hill, New York, 1964).
[36] J. Holtsmark, Ann. Physik (Wiley online) **363**, 577 (1919).
[37] G. Röpke and R. Der, Phys. Status Solidi B **92**, 501 (1979).